

1        ***Necator americanus Ancylostoma secreted protein-2 (Na-ASP-2) selectively binds an***  
2        ***ascaroside (ascr#3)***  
3

4        Ola El Atab<sup>1+</sup>, Rabih Darwiche<sup>1,2+</sup>, Nathanyal J. Truax<sup>3+</sup>, Roger Schneiter<sup>1</sup>, Kenneth G. Hull<sup>3</sup>,  
5        Daniel Romo<sup>3</sup> and Oluwatoyin A. Asojo<sup>4,5\*</sup>

6

7        <sup>1</sup>Division of Biochemistry, Department of Biology, University of Fribourg, Chemin du Musée 10,  
8        CH 1700 Fribourg, Switzerland

9        <sup>2</sup>Department of Biological Chemistry and Molecular Pharmacology, Harvard Medical School,  
10      Boston, MA 02115

11      <sup>3</sup>Department of Chemistry and Biochemistry & The CPRIT Synthesis and Drug-Lead Discovery  
12      Laboratory, Baylor University, One Bear Place, Waco, Texas 76798-7348, United States

13      <sup>4</sup>Department of Chemistry and Biochemistry, 200 William Harvey Way, Hampton University,  
14      Hampton VA, 23668

15      <sup>5</sup>National School of Tropical Medicine, Baylor College of Medicine, Houston Texas, 77030

16

17      <sup>+</sup> Equal contribution

18

19      \*To whom correspondence should be addressed

20

21      ***Running Title: Na-ASP-2 binds ascr#3***

22      **Keywords:** Venom allergen-like (VAL), sperm coating protein (SCP); TAPs [testis specific  
23      proteins (Tpx) / antigen 5 (Ag5) / pathogenesis related-1 (PR-1) / Sc7]; CAP [cysteine-rich  
24      secretory protein (CRISP) / antigen 5 / pathogenesis related-1 (PR-1)]; lipid binding; SCP/TAPS  
25      (Sperm-coating protein / Tpx / antigen 5 / pathogenesis related-1 / Sc7); ascarosides

26 Email and ORCID of authors  
27 Ola El Atab [ola.elatab@unifr.ch](mailto:ola.elatab@unifr.ch) 0000-0003-3118-0828  
28 Rabih Darwiche [Rabih\\_Darwiche@hms.harvard.edu](mailto:Rabih_Darwiche@hms.harvard.edu) 0000-0003-1909-4927  
29 Nathanyal J. Truax [Nathanyal\\_Truax1@baylor.edu](mailto:Nathanyal_Truax1@baylor.edu) 0000-0002-8510-2326  
30 Roger Schneiter [roger.schneiter@unifr.ch](mailto:roger.schneiter@unifr.ch) 0000-0002-9102-8396  
31 Kenneth G. Hull [Kenneth\\_Hull@baylor.edu](mailto:Kenneth_Hull@baylor.edu) 0000-0002-3697-9551  
32 Daniel Romo [Daniel\\_Romo@baylor.edu](mailto:Daniel_Romo@baylor.edu) 0000-0003-3805-092X  
33 Oluwatoyin A. Asojo [Oluwatoyin.asojo@hamptonu.edu](mailto:Oluwatoyin.asojo@hamptonu.edu) 0000-0002-4043-2700  
34  
35

### 36 **Abstract**

37 During their infective stages, hookworms release excretory-secretory (E-S) products, including  
38 small molecules and proteins, to help evade and suppress the host's immune system. Small  
39 molecules found in E-S products of mammalian hookworms include nematode derived metabolites  
40 like ascarosides, which are composed of the sugar ascaryllose linked to a fatty acid side chain.  
41 Ascarosides play vital roles in signaling, development, reproduction, and survival. The most  
42 abundant proteins found in hookworm E-S products are members of the protein family known as  
43 *Ancylostoma* secreted protein (ASP). ASP belongs to the SCP/TAPS (sperm-coating protein / Tpx  
44 / antigen 5 / pathogenesis related-1 / Sc7) superfamily of proteins, members of which have  
45 previously been shown to bind to eicosanoids and fatty acids. These molecules are structurally  
46 similar to the fatty acid moieties of ascarosides. The objective of this study was to determine if  
47 the hookworm ASP; *N. americanus* *Ancylostoma* secreted protein 2 (Na-ASP-2) binds to the  
48 ascarosides or their fatty acid moieties. We describe investigations of our hypothesis that there is

49 a functional relationship between the major secreted proteins and signaling small molecules found  
50 in hookworm E-S products. To accomplish this, several ascarosides and their fatty acid moieties  
51 were synthesized and tested for *in vitro* binding to *Na-ASP-2* using a ligand competition assay and  
52 microscale thermophoresis. Our results reveal that the fatty acid moieties of the ascarosides, bind  
53 specifically to the palmitic acid binding cavity of *Na-ASP-2*. Additionally, ascr#3, an ascaroside  
54 that is present in mammalian hookworm E-S products binds to the palmitic acid binding cavity of  
55 *Na-ASP-2*, whereas oscr#10 which is not found in hookworm E-S products does not bind. Future  
56 studies are required to determine the structural basis of ascaroside binding by *Na-ASP-2* and to  
57 understand the physiological significance of these observations.

58

59 **1. Introduction**

60 *Necator americanus* and *Ancylostoma duodenale* are hookworms that infect more than 400  
61 million of the world's poorest people causing a disease burden of over 22 million disability-  
62 adjusted life years (de Silva et al., 2003; Diemert et al., 2018; Hotez, 2007; Murray et al., 2014).  
63 During the transition to parasitism, the most abundant proteins secreted by third-stage infective  
64 larvae (L3) of *N. americanus* upon host entry are *N. americanus Ancylostoma* secreted protein 1  
65 (*Na-ASP-1*) and *N. americanus Ancylostoma* secreted protein 2 (*Na-ASP-2*) (Hotez et al., 2003).  
66 These *Ancylostoma* secreted protein sometimes referred to as VALs (venom allergen like) are the  
67 major protein components of the L3 excretory-secretory (E-S) products that facilitate the evasion  
68 and suppression of the host's immune system and have been found in all parasitic nematodes  
69 studied to date (Asojo et al., 2018; Darwiche et al., 2018; Gao et al., 2001; Hawdon and Hotez,  
70 1996; Hawdon et al., 1996; Hawdon et al., 1995; Hawdon et al., 1999; Zhan et al., 2003). ASPs  
71 belong to the SCP/TAPS (sperm-coating protein / Tpx / antigen 5 / pathogenesis related-1 / Sc7)

72 superfamily of proteins, NCBI domain cd00168 or Pfam PF00188 (Gibbs et al., 2008). SCP/TAPS  
73 proteins include plant PR-1 (pathogenesis-related 1) and CRISPs (cysteine-rich secretory protein),  
74 which are expressed in the mammalian reproductive tract, and venom allergens from insects and  
75 reptiles (Gibbs and O'Bryan, 2007; Gibbs et al., 2008; Gibbs et al., 2006). Members of the  
76 SCP/TAPS superfamily are also implicated in other biological phenomena including cellular  
77 defense such as plant responses to pathogens, sexual reproduction, and human brain tumor growth  
78 (Ding et al., 2000; Gao et al., 2001; Gibbs et al., 2010; Gibbs et al., 2008; Hawdon et al., 1999;  
79 Zhan et al., 2003).  
80 SCP/TAPS proteins have either one or two ~15 kDa cysteine-rich CAP domains (cysteine-rich  
81 secretory protein, antigen 5, and pathogenesis-related 1) as typified by the structures of *Na*-ASP-2  
82 (one CAP domain) and *Na*-ASP-1 (two covalently linked CAP domains) (Asojo, 2011; Asojo et  
83 al., 2005a; Asojo et al., 2011; Borloo et al., 2013; Fernandez et al., 1997; Gibbs et al., 2008; Guo  
84 et al., 2005; Serrano et al., 2004; Shikamoto et al., 2005; Wang et al., 2005; Xu et al., 2012). The  
85 CAP domain has an alpha-beta-alpha sandwich topology, and up to 50 % loop regions, which often  
86 makes it difficult to predict structure by homology modelling alone (Asojo et al., 2005a; Asojo et  
87 al., 2005b; Darwiche et al., 2016; Kelleher et al., 2014). The CAP domain has multiple cavities  
88 and verified ligand binding regions, and the first to be identified was a large central cavity that  
89 may contain a tetrad of residues, two His and two Glu that bind divalent cations including  $Zn^{2+}$   
90 and  $Mg^{2+}$  (Asojo et al., 2018; Asojo et al., 2011; Darwiche et al., 2018; Gibbs et al., 2008; Mason  
91 et al., 2014; Wang et al., 2010). Distinct lipid binding sites have been verified in SCP/TAPS  
92 proteins, including phosphatidylinositol binding regions on the surface of human golgi-associated  
93 plant pathogenesis-related protein 1 (GAPR-1) (Darwiche et al., 2016; van Galen et al., 2012; Van  
94 Galen et al., 2010; Xu et al., 2012). A sterol binding caveolin-binding motif (CBM) of the yeast

95 CAP proteins required for *in vivo* transport of cholesterol has also been identified in diverse  
96 SCP/TAPS proteins (Asojo et al., 2018; Choudhary et al., 2014; Darwiche et al., 2017a; Darwiche  
97 et al., 2016; Darwiche et al., 2018; Darwiche et al., 2017b; Kelleher et al., 2014). Furthermore, a  
98 hydrophobic channel that binds leukotrienes with sub-micromolar affinities, allows tablysin-15,  
99 an SCP/TAPS protein from the horsefly *Tabanus yao*, to function as an anti-inflammatory  
100 scavenger of eicosanoids (Xu et al., 2012). This binding cavity is formed by conserved central  
101 helices in SCP/TAPS proteins and also binds fatty acids, including palmitic acid (Xu et al., 2012).  
102 Our previous studies revealed that palmitic acid specifically binds to this cavity in other  
103 SCP/TAPS proteins including pathogen-related in yeast protein 1(Pry1) from *Saccharomyces*  
104 *cerevisiae* hence the cavity is referred to as the fatty acid-binding cavity (Asojo et al., 2018;  
105 Darwiche et al., 2016; Darwiche et al., 2018; Kelleher et al., 2014). While lipid binding had been  
106 confirmed for other parasite SCP/TAPS proteins, we solved the structure of *Na*-ASP-2 prior to the  
107 discovery of the lipid binding activity of members of this protein superfamily (Asojo et al., 2005a).  
108 The impetus for the current studies is to unravel possible lipid binding functions of *Na*-ASP-2.  
109 Our working hypothesis is that there is a functional relationship between small molecules and  
110 proteins secreted in hookworm E-S products. Thus, we are interested in the ability of *Na*-ASP-2  
111 to bind small molecules with known functions secreted by L3 hookworms. These small molecules  
112 include nematode derived metabolites notably the ascarosides which regulate a diverse range of  
113 phenotypes in nematodes including dauer arrest, mate attraction, aggregation and olfactory  
114 plasticity (Butcher et al., 2007; Choe et al., 2012; Gallo and Riddle, 2009; Hollister et al., 2013;  
115 Izrayelit et al., 2012; Jezyk and Fairbairn, 1967; Kaplan et al., 2011; Kunert, 1992; Ludewig and  
116 Schroeder, 2013; Noguez et al., 2012; Rhoads et al., 2015; Sakai et al., 2013; Tarr and Fairbairn,  
117 1973; Tarr and Schnoes, 1973). Ascarosides are multifunctional small molecules that interact with

118 G-protein-coupled receptors (GPCRs) (Butcher, 2017; Park et al., 2012). Ascarosides are  
119 composed of the sugar ascaroside linked to a fatty acid moiety (eg. ascr#3 (1) and oscr#10 (2),  
120 Figure 1) and while ascr#3 (1) was identified in the E-S products of mammalian hookworms,  
121 oscr#10 (2) was identified in other nematodes, but not hookworm (Choe et al., 2012; Gallo and  
122 Riddle, 2009; Hollister et al., 2013; Izrayelit et al., 2012; Jezyk and Fairbairn, 1967; Kaplan et al.,  
123 2011; Kunert, 1992; Ludewig and Schroeder, 2013; Noguez et al., 2012; Rhoads et al., 2015; Tarr  
124 and Fairbairn, 1973; Tarr and Schnoes, 1973). Since the fatty acid moieties of ascarosides are  
125 similar to those that are capable of binding to the fatty acid-binding cavity of ASPs, we carried out  
126 studies to determine if the ascarosides or their fatty acid moieties bind to *Na*-ASP-2.

127

128 **2. Experimental Procedures**

129 **2.1. Expression and purification of *Pry1* and *Na*-ASP-2**

130 DNA encoding for *Pry1* and *Na*-ASP-2 were PCR amplified and cloned into NcoI and XhoI  
131 restriction sites of pET22b vector (Novagen, Merck, Darmstadt, Germany), which contains a pelB  
132 signal sequence to direct the secretion of expressed protein into the periplasmic space. Plasmids  
133 were transformed into *Escherichia coli* BL21 and proteins were expressed with a C-terminal  
134 polyhistidine-tag. Protein expression was induced overnight with lactose at 24°C. Cells were  
135 collected, lysed and incubated with nickel-nitrilotriacetic acid beads as per the manufacturer  
136 instructions (Qiagen, Hilden, Germany). Beads were washed, loaded onto a Ni<sup>2+</sup>-NTA column and  
137 proteins were eluted in 60 mM NaH<sub>2</sub>PO<sub>4</sub>, 300 mM NaCl and 300 mM imidazole, pH 8.0. Prior to  
138 microscale thermophoresis experiments, proteins were applied to Zeba<sup>TM</sup> spin desalting columns  
139 (Thermo scientific) and the buffer was exchanged to 60 mM NaH<sub>2</sub>PO<sub>4</sub>, 300 mM NaCl, pH 8.0.  
140 Protein concentration was determined by Lowry assay using folin reagent and BSA as standard.

141

142 **2.2. *In vitro* radioligand lipid binding assay**

143 The radioligand binding assay was performed as described previously (Choudhary and  
144 Schneiter, 2012; Im et al., 2005). 100 pmol of purified untagged CAP protein (*Na*-ASP-2 or Pry1)  
145 in binding buffer (20 mM Tris, pH 7.5, 30 mM NaCl, 0.05% Triton X-100) was incubated for 1 h  
146 at 30 °C with different concentrations of either [<sup>3</sup>H]-cholesterol or [<sup>3</sup>H]-palmitic acid. Protein was  
147 removed from unbound ligand by adsorption to Q-sepharose beads (GE healthcare, USA), the  
148 beads were washed, protein was eluted and the protein-bound radioligand was quantified by  
149 scintillation counting. For competition binding assays, specified concentrations of unlabeled  
150 cholesterol, palmitic acid or ligands, were included in the binding reaction. Non-specific binding  
151 was determined by performing the assays without the addition of protein. Statistical significance  
152 of data was analyzed by multiple t-test (GraphPad Prism, La Jolla, CA).

153

154 **2.3. Microscale Thermophoresis**

155 Microscale thermophoresis was performed using a Monolith NT.115 from Nanotemper  
156 Technologies (Munich, Germany) (Seidel et al., 2012; Shang et al., 2012; Zillner et al., 2012). His-  
157 tagged protein (Pry1 or *Na*-ASP-2) was fluorescently labeled using the RED-tris-NTA His tag  
158 protein labeling kit (Nanotemper Technologies). Labeled protein (Pry1 or *Na*-ASP-2) was  
159 subsequently added to serial dilution of unlabeled ligand (ascarosides or their fatty acid moieties)  
160 in binding buffer (20 mM Tris pH 7.5, 30 mM NaCl, 0.05% Triton X-100). Each sample was  
161 loaded into standard glass capillaries, and measurements were performed at 60% power setting.  
162 The dissociation constant Kd was obtained by plotting the normalized fluorescence (Fnorm)  
163 against the logarithm of ligand concentration. Experiments were performed in triplicates and data

164 were fitted using the Kd model with the MO.Affinity Analysis software (Nanotemper  
165 Technologies, Munich, Germany).

166

167 **2.4. Synthesis of Ascarosides and ligands**

168 Benzoyl protected ascarylose **8** was prepared as previously reported by Jeong and co-workers from  
169 commercially available L-rhamnose **6** (Jeong et al., 2005) with the exception of a modified final  
170 reduction (Figure 2). The previously reported reduction of lactone **7** with disiamyl borane (Jeong  
171 et al., 2005) proved irreproducible in our hands, resulting in incomplete conversion and low overall  
172 yields (~40 %). Thus, an alternative was identified involving reduction with 9-BBN to provide the  
173 desired lactol **7** in improved yield (70 %). With protected ascarylose **8** in hand, we next studied  
174 glycosylation at C1 to append the fatty acid side chain present in the targeted ascarosides. Previous  
175 synthetic strategies to these targets involved glycosylation of secondary alcohols bearing long  
176 alkyl chains with a terminal alkene which was subsequently utilized for late stage cross metathesis  
177 or oxidations (Butcher et al., 2009; Hollister et al., 2013; Jeong et al., 2005; Martin et al., 2009;  
178 Noguez et al., 2012; Srinivasan et al., 2012). Since we intended to study the binding affinity of  
179 the natural ascarocides and their intact fatty acid moieties independently, we decided to first  
180 synthesize intact fatty acid side moieties **9** and **11** and then couple them directly to protected  
181 ascarylose **8** during the penultimate step of the sequence. This strategy provided rapid access to  
182 ascarosides **1** and **2** along with fatty acid derivatives **3-5** for screening. Subsequent Lewis acid-  
183 mediated glycosylation with  $\text{BF}_3\text{-Et}_2\text{O}$  of fatty acid **9** (see SI for synthetic details) and  
184 commercially available acid **11** (Jeong et al., 2005) proceeded uneventfully and provided protected  
185 ascarosides **10** and **12** in 68 and 66% yield, respectively. Subsequent global deprotection with  
186 lithium hydroxide gave ascr#3 (**1**) and oscr#10 (**2**).

187

188 **3. Results**

189 **3.1. *Na-ASP-2 binds cholesterol and palmitic acid *in vitro****

190 The *in vitro* cholesterol-binding activity of *Na-ASP-2* was examined using increasing  
191 concentrations of radiolabeled [<sup>3</sup>H]-cholesterol and a constant concentration of purified protein.  
192 *Na-ASP-2* displayed saturable binding of cholesterol with an apparent dissociation constant  $K_d$  of  
193 2.1  $\mu$ M (Figure 3A). *Na-ASP-2* has similar cholesterol binding affinity as reported for other  
194 SCP/TAPS family members from yeast, *Saccharomyces cerevisiae* (Pry1, 1.9  $\mu$ M), *Brugia malayi*  
195 (*Bm*-VAL-1, 0.9  $\mu$ M), *Heligmosomoides polygyrus* (Hp-VAL-4, 1.53  $\mu$ M) and *Schistosoma*  
196 *mansi* (*Sm*-VAL-4, 2.4  $\mu$ M) (Asojo et al., 2018; Darwiche et al., 2016; Darwiche et al., 2018;  
197 Kelleher et al., 2014). Furthermore, addition of equimolar or excess concentration of unlabeled  
198 cholesterol reduced binding of the radioligand, indicating that binding is specific as shown in  
199 Figure 3A,B.

200 Tablycin-15, a horsefly SCP/TAPS protein was shown to bind fatty acids with a  
201 hydrophobic pocket formed between two central helices (Ma et al., 2011). This hydrophobic  
202 pocket is observed in other SCP/TAPS proteins and we previously confirmed the ability of these  
203 proteins to bind palmitic acid *in vitro* (Asojo et al., 2018; Darwiche et al., 2016; Darwiche et al.,  
204 2018; Kelleher et al., 2014). To examine whether *Na-ASP-2* can bind palmitic acid, we carried  
205 out direct binding studies using [<sup>3</sup>H]-palmitic acid as radiolabeled ligand, as shown in Figure 3C.  
206 *Na-ASP-2* showed a saturable binding for palmitic acid with an apparent  $K_d$  of 95  $\mu$ M, which is of  
207 the same magnitude as previously measured for the SCP/TAPS family members from yeast (Pry1,  
208  $K_d$  = 112  $\mu$ M), *Brugia malayi* (*Bm*-VAL-1,  $K_d$  = 83  $\mu$ M), and comparable to tablycin-15 ( $K_d$  = 94  
209  $\mu$ M) (Asojo et al., 2018; Darwiche et al., 2016; Darwiche et al., 2018; Kelleher et al., 2014). For

210 competition binding assays, binding of *Na*-ASP-2 to palmitic acid was reduced in the presence of  
211 unlabeled palmitic acid, indicating that binding is specific (Figure 3C, D). Taken together our  
212 results indicate that *Na*-ASP-2 binds cholesterol and palmitic acid *in vitro*.

213

214 **3.2. Fatty acids and ascaroside binding is selective for the palmitate-binding cavity**

215 Having confirmed the ability of *Na*-ASP-2 to bind cholesterol, we carried out competitive  
216 binding studies of ascarosides and their fatty acid moieties against radiolabeled cholesterol. At a  
217 concentration of 50 pmol, the typical concentration for our cholesterol binding assay, neither  
218 ascarosides (ascr#3 (1) and oscr#10 (2)) nor fatty acids (3-5) competed with the radiolabelled  
219 [<sup>3</sup>H]-cholesterol (50 pmol) for binding to *Na*-ASP-2 (Figure 4A). We also tested if the ascarosides  
220 or their fatty acid moieties bind to the fatty acid binding cavity. Our studies showed that the  
221 binding of [<sup>3</sup>H]-palmitic acid by *Na*-ASP-2 was competed by the ascaroside, ascr#3 (1) and by all  
222 the fatty acid moieties 3-5 tested with the same order of magnitude, but not by the ascaroside,  
223 oscr#10 (2) (Figure 4B). We tested the ability of Pry1, a SCP/TAPS protein from *S. cerevisiae*,  
224 an organism that does not contain ascarosides, to bind to the same ligands. Our analysis revealed  
225 that while the fatty acids (3-5) competed for palmitic acid binding to Pry1, neither ascr#3 (1) nor  
226 oscr#10 (2) bound to Pry1. Furthermore, addition of excess ligands (fatty acids (3-5)) competed  
227 with radioligand binding while binding of [<sup>3</sup>H]-palmitic acid to Pry1 could not be competed for by  
228 the addition of excess unlabeled ascr#3 (1) or oscr#10 (2) (Figure 4C). We independently validated  
229 the binding of ligands to Pry1 and *Na*-ASP-2 by microscale thermophoresis and determined  
230 binding constants (Figure 5). The results of these analyses confirmed that Pry1 does not bind  
231 ascr#3 or oscr#10, but it binds palmitic acid and the fatty acid moieties present in ascarosides. *Na*-  
232 ASP-2, on the other hand, bound ascr#3 (1) with a  $K_d$  of 142  $\mu$ M but did not bind oscr#10 (2),

233 which is consistent with the results obtained by the ligand competition assay and indicates that *Na-*  
234 *ASP-2* binds ascr#3 (**1**) through its fatty-acid binding pocket.

235

236 **4. Discussion**

237 We present here efficient methods to synthesize the ascarocides and their fatty acid  
238 moieties. We also present data revealing that the fatty acid moieties of ascarosides compete for  
239 binding to the palmitate-binding cavities of both *Pry1* and *Na-ASP-2* but as expected do not bind  
240 to the sterol binding cavity. The micromolar binding affinity of ascr#3 and free fatty acids are  
241 comparable to that observed for palmitic acid to the palmitate-binding cavity of other CAP  
242 proteins. While it is unclear if ascr#3 binding is physiologically relevant, the finding that ascr#3  
243 (**1**) binds *Na-ASP-2* is still interesting considering that a high relative abundance of ascr#3 (**1**) was  
244 detected in E-S products from both the infective juvenile and adult stages of *Nippostrongylus*  
245 *brasiliensis* by HPLC-MS(Choe et al., 2012). It is plausible that ascr#3 (**1**) is present in human  
246 hookworms since there appears to be a conservation of ascaroside production in families of  
247 nematodes (Choe et al., 2012). A blast search of the *Na-ASP-2* sequence against the *N. brasiliensis*  
248 proteins reveals several SCP/TAPs proteins, which share over 45 % sequence similarity with *Na-*  
249 *ASP-2*. Even more remarkable, the residues and predicted structures of the helical regions notably  
250 residues corresponding to (alpha 1 and alpha 3) that form the fatty acid-binding cavity are  
251 conserved (Figure 6A). This structural similarity suggests that these proteins likely behave  
252 similarly to *Na-ASP-2* as we observed previously for the orthologues from *B. malayi* and *H.*  
253 *polygyrus*. Additionally, we observed that the incorporation of the ascarylose sugar abrogated the  
254 ability of these fatty acids to bind to *Pry1*. A comparison of the helices bordering the palmitic acid  
255 binding cavities of *Pry1* and *Na-ASP-2* reveals that *Pry1* has shorter helices than *Na-ASP-2*, which

256 results in a smaller hydrophobic binding pocket in Pry1 compared to *Na*-ASP-2 (Figures 6A and  
257 B). This smaller size may explain the failure of Pry1 to accommodate ascaroside as opposed to  
258 free fatty acids. The inability of *Na*-ASP-2 to bind oscr#10 (2) cannot be explained by the size  
259 difference of the cavities and suggests a new hypothesis that we plan to test in future; that  
260 ascaroside binding may be specific for certain SCP/TAPS proteins, indicating a possible functional  
261 relationship between ascarosides and parasite SCP/TAPS proteins.

262

263 **5. Conclusions**

264 In summary, our results reveal that the fatty acid moieties of the ascarosides, ascr#3 (1)  
265 and oscr#10 (2), bind specifically to the fatty acid binding cavity of both *Na*-ASP-2 and Pry1, with  
266 the latter protein from *Saccharomyces cerevisiae* SCP/TAPS serving as a control. Additionally,  
267 ascr#3 (1), an ascaroside that is present in mammalian hookworm E-S products binds  
268 competitively to the fatty acid binding cavity of *Na*-ASP-2, whereas oscr#10 (2) which is not found  
269 in hookworm E-S products did not. Interestingly, neither ascaroside bound to Pry1. Studies to  
270 identify how ascarosides precisely interact with parasite CAP proteins are currently underway.  
271 More studies need to be conducted to determine the physiological relevance of the fatty acid-  
272 binding cavity of *Na*-ASP-2.

273

274

275 **Acknowledgments**

276 RS thanks the Swiss National Science Foundation for support (grant 31003A\_173003). This study  
277 was supported in part by funds from the Collaborative Faculty Research Investment Program of  
278 Baylor University, Baylor Scott & White Health and Baylor College of Medicine to OAA and DR.

279

280 **Author Contributions Statement**

281 Designed the studies: OAA, OEA, RS, RD, KDH, DR

282 Conducted experiments: OEA, RD, NJT

283 All authors contributed expertise and to the final manuscript.

284

285

286 **References**

287

288 Asojo, O.A., 2011. Crystal Structure of a two-CAP domain protein from the human hookworm  
289 parasite *Necator americanus*. *Acta Cryst Sect D* 455-462.

290

291 Asojo, O.A., Darwiche, R., Gebremedhin, S., Smant, G., Lozano-Torres, J.L., Drurey, C., Pollet,  
292 J., Maizels, R.M., Schneiter, R., Wilbers, R.H.P., 2018. *Heligmosomoides polygyrus* Venom  
293 Allergen-like Protein-4 (HpVAL-4) is a sterol binding protein. *Int J Parasitol* 48, 359-369.

294

295 Asojo, O.A., Goud, G., Dhar, K., Loukas, A., Zhan, B., Deumic, V., Liu, S., Borgstahl, G.E.,  
296 Hotez, P.J., 2005a. X-ray structure of Na-ASP-2, a pathogenesis-related-1 protein from the  
297 nematode parasite, *Necator americanus*, and a vaccine antigen for human hookworm infection. *J*  
298 *Mol Biol* 346, 801-814.

299

300 Asojo, O.A., Koski, R.A., Bonafe, N., 2011. Structural studies of human glioma pathogenesis-  
301 related protein 1. *Acta crystallographica. Section D, Biological crystallography* 67, 847-855.

302

303 Asojo, O.A., Loukas, A., Inan, M., Barent, R., Huang, J., Plantz, B., Swanson, A., Gouthro, M.,  
304 Meagher, M.M., Hotez, P.J., 2005b. Crystallization and preliminary X-ray analysis of Na-ASP-1,  
305 a multi-domain pathogenesis-related-1 protein from the human hookworm parasite *Necator*  
306 *americanus*. *Acta Crystallograph Sect F Struct Biol Cryst Commun* 61, 391-394.

307

308 Borloo, J., Geldhof, P., Peelaers, I., Van Meulder, F., Ameloot, P., Callewaert, N., Vercruyse, J.,  
309 Claerebout, E., Strelkov, S.V., Weeks, S.D., 2013. Structure of *Ostertagia ostertagi* ASP-1:  
310 insights into disulfide-mediated cyclization and dimerization. *Acta crystallographica. Section D,*  
311 *Biological crystallography* 69, 493-503.

312

313 Butcher, R.A., 2017. Decoding chemical communication in nematodes. *Nat Prod Rep* 34, 472-  
314 477.

315

316 Butcher, R.A., Fujita, M., Schroeder, F.C., Clardy, J., 2007. Small-molecule pheromones that  
317 control dauer development in *Caenorhabditis elegans*. *Nat Chem Biol* 3, 420-422.

318

319 Butcher, R.A., Ragains, J.R., Clardy, J., 2009. An indole-containing dauer pheromone component  
320 with unusual dauer inhibitory activity at higher concentrations. *Org Lett* 11, 3100-3103.

321

322 Choe, A., von Reuss, S.H., Kogan, D., Gasser, R.B., Platzer, E.G., Schroeder, F.C., Sternberg,  
323 P.W., 2012. Ascaroside signaling is widely conserved among nematodes. *Curr Biol* 22, 772-780.

324

325 Choudhary, V., Darwiche, R., Gfeller, D., Zoete, V., Michielin, O., Schneiter, R., 2014. The  
326 caveolin-binding motif of the pathogen-related yeast protein Pry1, a member of the CAP protein  
327 superfamily, is required for in vivo export of cholesteryl acetate. *Journal of lipid research* 55, 883-  
328 894.

329

330 Choudhary, V., Schneiter, R., 2012. Pathogen-Related Yeast (PRY) proteins and members of the  
331 CAP superfamily are secreted sterol-binding proteins. *Proceedings of the National Academy of  
332 Sciences of the United States of America* 109, 16882-16887.

333

334 Darwiche, R., El Atab, O., Cottier, S., Schneiter, R., 2017a. The function of yeast CAP family  
335 proteins in lipid export, mating, and pathogen defense. *FEBS Lett.*

336

337 Darwiche, R., Kelleher, A., Hudspeth, E.M., Schneiter, R., Asojo, O.A., 2016. Structural and  
338 functional characterization of the CAP domain of pathogen-related yeast 1 (Pry1) protein. *Sci Rep*  
339 6, 28838.

340

341 Darwiche, R., Lugo, F., Drurey, C., Varossieau, K., Smant, G., Wilbers, R.H.P., Maizels, R.M.,  
342 Schneiter, R., Asojo, O.A., 2018. Crystal structure of *Brugia malayi* venom allergen-like protein-  
343 1 (BmVAL-1), a vaccine candidate for lymphatic filariasis. *Int J Parasitol* 48, 371-378.

344

345 Darwiche, R., Mene-Saffrane, L., Gfeller, D., Asojo, O.A., Schneiter, R., 2017b. The pathogen-  
346 related yeast protein Pry1, a member of the CAP protein superfamily, is a fatty acid-binding  
347 protein. *J Biol Chem.*

348

349 de Silva, N.R., Brooker, S., Hotez, P.J., Montresor, A., Engels, D., Savioli, L., 2003. Soil-  
350 transmitted helminth infections: updating the global picture. *Trends Parasitol* 19, 547-551.

351 Diemert, D., Campbell, D., Brelsford, J., Leasure, C., Li, G., Peng, J., Zumer, M., Younes, N.,  
352 Bottazzi, M.E., Mejia, R., Pritchard, D.I., Hawdon, J.M., Bethony, J.M., 2018. Controlled Human  
353 Hookworm Infection: Accelerating Human Hookworm Vaccine Development. *Open Forum Infect  
354 Dis* 5, ofy083.

355

356 Ding, X., Shields, J., Allen, R., Hussey, R.S., 2000. Molecular cloning and characterisation of a  
357 venom allergen AG5-like cDNA from *Meloidogyne incognita*. *Int J Parasitol* 30, 77-81.

358

359 Fernandez, C., Szyperski, T., Bruyere, T., Ramage, P., Mosinger, E., Wuthrich, K., 1997. NMR  
360 solution structure of the pathogenesis-related protein P14a. *J Mol Biol* 266, 576-593.

361

362 Gallo, M., Riddle, D.L., 2009. Effects of a *Caenorhabditis elegans* dauer pheromone ascaroside on  
363 physiology and signal transduction pathways. *J Chem Ecol* 35, 272-279.

364

365 Gao, B., Allen, R., Maier, T., Davis, E.L., Baum, T.J., Hussey, R.S., 2001. Molecular  
366 characterisation and expression of two venom allergen-like protein genes in *Heterodera glycines*.  
367 *Int J Parasitol* 31, 1617-1625.

368

369 Gibbs, G.M., Lo, J.C., Nixon, B., Jamsai, D., O'Connor, A.E., Rijal, S., Sanchez-Partida, L.G.,  
370 Hearn, M.T., Bianco, D.M., O'Bryan, M.K., 2010. Glioma pathogenesis-related 1-like 1 is testis  
371 enriched, dynamically modified, and redistributed during male germ cell maturation and has a  
372 potential role in sperm-oocyte binding. *Endocrinology* 151, 2331-2342.

373

374 Gibbs, G.M., O'Bryan, M.K., 2007. Cysteine rich secretory proteins in reproduction and venom.  
375 *Soc Reprod Fertil Suppl* 65, 261-267.

376

377 Gibbs, G.M., Roelants, K., O'Bryan, M.K., 2008. The CAP superfamily: cysteine-rich secretory  
378 proteins, antigen 5, and pathogenesis-related 1 proteins--roles in reproduction, cancer, and immune  
379 defense. *Endocr Rev* 29, 865-897.

380

381 Gibbs, G.M., Scanlon, M.J., Swarbrick, J., Curtis, S., Gallant, E., Dulhunty, A.F., O'Bryan, M.K.,  
382 2006. The cysteine-rich secretory protein domain of Tpx-1 is related to ion channel toxins and  
383 regulates ryanodine receptor Ca<sup>2+</sup> signaling. *J Biol Chem* 281, 4156-4163.

384

385 Gouet, P., Robert, X., Courcelle, E., 2003. ESPript/ENDscript: Extracting and rendering sequence  
386 and 3D information from atomic structures of proteins. *Nucleic Acids Res* 31, 3320-3323.

387

388 Guo, M., Teng, M., Niu, L., Liu, Q., Huang, Q., Hao, Q., 2005. Crystal structure of the cysteine-  
389 rich secretory protein stecrisp reveals that the cysteine-rich domain has a K<sup>+</sup> channel inhibitor-  
390 like fold. *J Biol Chem* 280, 12405-12412.

391

392 Hawdon, J.M., Hotez, P.J., 1996. Hookworm: developmental biology of the infectious process.  
393 *Curr Opin Genet Dev* 6, 618-623.

394

395 Hawdon, J.M., Jones, B.F., Hoffman, D.R., Hotez, P.J., 1996. Cloning and characterization of  
396 Ancylostoma-secreted protein. A novel protein associated with the transition to parasitism by  
397 infective hookworm larvae. *J Biol Chem* 271, 6672-6678.

398

399 Hawdon, J.M., Jones, B.F., Hotez, P.J., 1995. Cloning and characterization of a cDNA encoding  
400 the catalytic subunit of a cAMP-dependent protein kinase from *Ancylostoma caninum* third-stage  
401 infective larvae. *Mol Biochem Parasitol* 69, 127-130.

402

403 Hawdon, J.M., Narasimhan, S., Hotez, P.J., 1999. *Ancylostoma* secreted protein 2: cloning and  
404 characterization of a second member of a family of nematode secreted proteins from *Ancylostoma*  
405 *caninum*. *Mol Biochem Parasitol* 99, 149-165.

406

407 Hollister, K.A., Conner, E.S., Zhang, X., Spell, M., Bernard, G.M., Patel, P., de Carvalho, A.C.,  
408 Butcher, R.A., Ragains, J.R., 2013. Ascaroside activity in *Caenorhabditis elegans* is highly  
409 dependent on chemical structure. *Bioorg Med Chem* 21, 5754-5769.

410

411 Hotez, P.J., 2007. Neglected diseases and poverty in "The Other America": the greatest health  
412 disparity in the United States? *PLoS Negl Trop Dis* 1, e149.

413

414 Hotez, P.J., Zhan, B., Bethony, J.M., Loukas, A., Williamson, A., Goud, G.N., Hawdon, J.M.,  
415 Dobardzic, A., Dobardzic, R., Ghosh, K., Bottazzi, M.E., Mendez, S., Zook, B., Wang, Y., Liu,  
416 S., Essiet-Gibson, I., Chung-Debose, S., Xiao, S., Knox, D., Meagher, M., Inan, M., Correa-  
417 Oliveira, R., Vilk, P., Shepherd, H.R., Brandt, W., Russell, P.K., 2003. Progress in the  
418 development of a recombinant vaccine for human hookworm disease: the Human Hookworm  
419 Vaccine Initiative. *Int J Parasitol* 33, 1245-1258.

420

421 Im, Y.J., Raychaudhuri, S., Prinz, W.A., Hurley, J.H., 2005. Structural mechanism for sterol  
422 sensing and transport by OSBP-related proteins. *Nature* 437, 154-158.

423

424 Izrayelit, Y., Srinivasan, J., Campbell, S.L., Jo, Y., von Reuss, S.H., Genoff, M.C., Sternberg,  
425 P.W., Schroeder, F.C., 2012. Targeted metabolomics reveals a male pheromone and sex-specific  
426 ascaroside biosynthesis in *Caenorhabditis elegans*. *ACS Chem Biol* 7, 1321-1325.

427

428 Jeong, P.Y., Jung, M., Yim, Y.H., Kim, H., Park, M., Hong, E., Lee, W., Kim, Y.H., Kim, K.,  
429 Paik, Y.K., 2005. Chemical structure and biological activity of the *Caenorhabditis elegans* dauer-  
430 inducing pheromone. *Nature* 433, 541-545.

431

432 Jezyk, P.F., Fairbairn, D., 1967. Ascarosides and ascaroside esters in *Ascaris lumbricoides*  
433 (Nematoda). *Comp Biochem Physiol* 23, 691-705.

434

435 Kaplan, F., Srinivasan, J., Mahanti, P., Ajredini, R., Durak, O., Nimalendran, R., Sternberg, P.W.,  
436 Teal, P.E., Schroeder, F.C., Edison, A.S., Alborn, H.T., 2011. Ascaroside expression in  
437 *Caenorhabditis elegans* is strongly dependent on diet and developmental stage. PLoS One 6,  
438 e17804.

439

440 Kelleher, A., Darwiche, R., Rezende, W.C., Farias, L.P., Leite, L.C., Schneiter, R., Asojo, O.A.,  
441 2014. *Schistosoma mansoni* venom allergen-like protein 4 (SmVAL4) is a novel lipid-binding  
442 SCP/TAPS protein that lacks the prototypical CAP motifs. Acta crystallographica. Section D,  
443 Biological crystallography 70, 2186-2196.

444

445 Kunert, J., 1992. On the mechanism of penetration of ovicidal fungi through egg-shells of parasitic  
446 nematodes. Decomposition of chitinous and ascaroside layers. Folia Parasitol (Praha) 39, 61-66.

447

448 Ludewig, A.H., Schroeder, F.C., 2013. Ascaroside signaling in *C. elegans*. WormBook, 1-22.

449

450 Ma, D., Xu, X., An, S., Liu, H., Yang, X., Andersen, J.F., Wang, Y., Tokumasu, F., Ribeiro, J.M.,  
451 Francischetti, I.M., Lai, R., 2011. A novel family of RGD-containing disintegrins (Tablysin-15)  
452 from the salivary gland of the horsefly *Tabanus yao* targets alphaIIbbeta3 or alphaVbeta3 and  
453 inhibits platelet aggregation and angiogenesis. Thromb Haemost 105, 1032-1045.

454

455 Martin, R., Schmidt, A.W., Theumer, G., Krause, T., Entchev, E.V., Kurzchalia, T.V., Knolker,  
456 H.J., 2009. Synthesis and biological activity of the (25R)-cholesten-26-oic acids--ligands for the  
457 hormonal receptor DAF-12 in *Caenorhabditis elegans*. Org Biomol Chem 7, 909-920.

458

459 Mason, L., Tribolet, L., Simon, A., von Gnielinski, N., Nienaber, L., Taylor, P., Willis, C., Jones,  
460 M.K., Sternberg, P.W., Gasser, R.B., Loukas, A., Hofmann, A., 2014. Probing the equatorial  
461 groove of the hookworm protein and vaccine candidate antigen, Na-ASP-2. The international  
462 journal of biochemistry & cell biology 50, 146-155.

463

464 Murray, C.J., Ortblad, K.F., Guinovart, C., Lim, S.S., Wolock, T.M., Roberts, D.A., Dansereau,  
465 E.A., Graetz, N., Barber, R.M., Brown, J.C., Wang, H., Duber, H.C., Naghavi, M., Dicker, D.,  
466 Dandona, L., Salomon, J.A., Heuton, K.R., Foreman, K., Phillips, D.E., Fleming, T.D., Flaxman,  
467 A.D., Phillips, B.K., Johnson, E.K., Coggeshall, M.S., Abd-Allah, F., Abera, S.F., Abraham, J.P.,  
468 Abubakar, I., Abu-Raddad, L.J., Abu-Rmeileh, N.M., Achoki, T., Adeyemo, A.O., Adou, A.K.,  
469 Adsuar, J.C., Agardh, E.E., Akena, D., Al Kahbouri, M.J., Alasfoor, D., Albittar, M.I., Alcalá-  
470 Cerra, G., Alegretti, M.A., Alemu, Z.A., Alfonso-Cristancho, R., Alhabib, S., Ali, R., Alla, F.,  
471 Allen, P.J., Alsharif, U., Alvarez, E., Alvis-Guzman, N., Amankwaa, A.A., Amare, A.T., Amini,  
472 H., Ammar, W., Anderson, B.O., Antonio, C.A., Anwari, P., Arnlov, J., Arsenijevic, V.S.,  
473 Artaman, A., Asghar, R.J., Assadi, R., Atkins, L.S., Badawi, A., Balakrishnan, K., Banerjee, A.,  
474 Basu, S., Beardsley, J., Bekele, T., Bell, M.L., Bernabe, E., Beyene, T.J., Bhala, N., Bhalla, A.,

475 Bhutta, Z.A., Abdulhak, A.B., Binagwaho, A., Blore, J.D., Basara, B.B., Bose, D., Brainin, M.,  
476 Breitborde, N., Castaneda-Orjuela, C.A., Catala-Lopez, F., Chadha, V.K., Chang, J.C., Chiang,  
477 P.P., Chuang, T.W., Colomar, M., Cooper, L.T., Cooper, C., Courville, K.J., Cowie, B.C., Criqui,  
478 M.H., Dandona, R., Dayama, A., De Leo, D., Degenhardt, L., Del Pozo-Cruz, B., Deribe, K., Des  
479 Jarlais, D.C., Dessaegn, M., Dharmaratne, S.D., Dilmen, U., Ding, E.L., Driscoll, T.R., Durrani,  
480 A.M., Ellenbogen, R.G., Ermakov, S.P., Esteghamati, A., Faraon, E.J., Farzadfar, F.,  
481 Fereshtehnejad, S.M., Fijabi, D.O., Forouzanfar, M.H., Fra Paleo, U., Gaffikin, L., Gamkrelidze,  
482 A., Gankpe, F.G., Geleijnse, J.M., Gessner, B.D., Gibney, K.B., Ginawi, I.A., Glaser, E.L., Gona,  
483 P., Goto, A., Gouda, H.N., Gugnani, H.C., Gupta, R., Gupta, R., Hafezi-Nejad, N., Hamadeh, R.R.,  
484 Hammami, M., Hankey, G.J., Harb, H.L., Haro, J.M., Havmoeller, R., Hay, S.I., Hedayati, M.T.,  
485 Pi, I.B., Hoek, H.W., Hornberger, J.C., Hosgood, H.D., Hotez, P.J., Hoy, D.G., Huang, J.J., Iburg,  
486 K.M., Idrisov, B.T., Innos, K., Jacobsen, K.H., Jeemon, P., Jensen, P.N., Jha, V., Jiang, G., Jonas,  
487 J.B., Juel, K., Kan, H., Kankindi, I., Karam, N.E., Karch, A., Karema, C.K., Kaul, A., Kawakami,  
488 N., Kazi, D.S., Kemp, A.H., Kengne, A.P., Keren, A., Kereselidze, M., Khader, Y.S., Khalifa,  
489 S.E., Khan, E.A., Khang, Y.H., Khonelidze, I., Kinfu, Y., Kinge, J.M., Knibbs, L., Kokubo, Y.,  
490 Kosen, S., Defo, B.K., Kulkarni, V.S., Kulkarni, C., Kumar, K., Kumar, R.B., Kumar, G.A., Kwan,  
491 G.F., Lai, T., Balaji, A.L., Lam, H., Lan, Q., Lansingh, V.C., Larson, H.J., Larsson, A., Lee, J.T.,  
492 Leigh, J., Leinsalu, M., Leung, R., Li, Y., Li, Y., De Lima, G.M., Lin, H.H., Lipshultz, S.E., Liu,  
493 S., Liu, Y., Lloyd, B.K., Lotufo, P.A., Machado, V.M., Maclachlan, J.H., Magis-Rodriguez, C.,  
494 Majdan, M., Mapoma, C.C., Marcenes, W., Marzan, M.B., Masci, J.R., Mashal, M.T., Mason-  
495 Jones, A.J., Mayosi, B.M., Mazorodze, T.T., McKay, A.C., Meaney, P.A., Mehndiratta, M.M.,  
496 Mejia-Rodriguez, F., Melaku, Y.A., Memish, Z.A., Mendoza, W., Miller, T.R., Mills, E.J.,  
497 Mohammad, K.A., Mokdad, A.H., Mola, G.L., Monasta, L., Montico, M., Moore, A.R., Mori, R.,  
498 Moturi, W.N., Mukaigawara, M., Murthy, K.S., Naheed, A., Naidoo, K.S., Naldi, L., Nangia, V.,  
499 Narayan, K.M., Nash, D., Nejjari, C., Nelson, R.G., Neupane, S.P., Newton, C.R., Ng, M., Nisar,  
500 M.I., Nolte, S., Norheim, O.F., Nowaseb, V., Nyakarahuka, L., Oh, I.H., Ohkubo, T., Olusanya,  
501 B.O., Omer, S.B., Opio, J.N., Orisakwe, O.E., Pandian, J.D., Papachristou, C., Caicedo, A.J.,  
502 Patten, S.B., Paul, V.K., Pavlin, B.I., Pearce, N., Pereira, D.M., Pervaiz, A., Pesudovs, K., Petzold,  
503 M., Pourmalek, F., Qato, D., Quezada, A.D., Quistberg, D.A., Rafay, A., Rahimi, K., Rahimi-  
504 Movagh, V., Ur Rahman, S., Raju, M., Rana, S.M., Razavi, H., Reilly, R.Q., Remuzzi, G.,  
505 Richardus, J.H., Ronfani, L., Roy, N., Sabin, N., Saeedi, M.Y., Sahraian, M.A., Samonte, G.M.,  
506 Sawhney, M., Schneider, I.J., Schwebel, D.C., Seedat, S., Sepanlou, S.G., Servan-Mori, E.E.,  
507 Sheikbahaei, S., Shibuya, K., Shin, H.H., Shiue, I., Shivakoti, R., Sigfusdottir, I.D., Silberberg,  
508 D.H., Silva, A.P., Simard, E.P., Singh, J.A., Skirbekk, V., Sliwa, K., Soneji, S., Soshnikov, S.S.,  
509 Sreeramareddy, C.T., Stathopoulou, V.K., Stroumpoulis, K., Swaminathan, S., Sykes, B.L., Tabb,  
510 K.M., Talongwa, R.T., Tenkorang, E.Y., Terkawi, A.S., Thomson, A.J., Thorne-Lyman, A.L.,  
511 Towbin, J.A., Traebert, J., Tran, B.X., Dimbuene, Z.T., Tsilimbaris, M., Uchendu, U.S., Ukwaja,  
512 K.N., Uzun, S.B., Vallely, A.J., Vasankari, T.J., Venketasubramanian, N., Violante, F.S., Vlassov,  
513 V.V., Vollset, S.E., Waller, S., Wallin, M.T., Wang, L., Wang, X., Wang, Y., Weichenthal, S.,  
514 Weiderpass, E., Weintraub, R.G., Westerman, R., White, R.A., Wilkinson, J.D., Williams, T.N.,

515 Woldeyohannes, S.M., Wong, J.Q., Xu, G., Yang, Y.C., Yano, Y., Yentur, G.K., Yip, P.,  
516 Yonemoto, N., Yoon, S.J., Younis, M., Yu, C., Jin, K.Y., El Sayed Zaki, M., Zhao, Y., Zheng, Y.,  
517 Zhou, M., Zhu, J., Zou, X.N., Lopez, A.D., Vos, T., 2014. Global, regional, and national incidence  
518 and mortality for HIV, tuberculosis, and malaria during 1990-2013: a systematic analysis for the  
519 Global Burden of Disease Study 2013. *Lancet* 384, 1005-1070.  
520

521 Noguez, J.H., Conner, E.S., Zhou, Y., Ciche, T.A., Ragains, J.R., Butcher, R.A., 2012. A novel  
522 ascaroside controls the parasitic life cycle of the entomopathogenic nematode *Heterorhabditis*  
523 *bacteriophora*. *ACS Chem Biol* 7, 961-966.  
524

525 Park, D., O'Doherty, I., Somvanshi, R.K., Bethke, A., Schroeder, F.C., Kumar, U., Riddle, D.L.,  
526 2012. Interaction of structure-specific and promiscuous G-protein-coupled receptors mediates  
527 small-molecule signaling in *Caenorhabditis elegans*. *Proceedings of the National Academy of  
528 Sciences of the United States of America* 109, 9917-9922.  
529

530 Rhoads, T.W., Prasad, A., Kwiecien, N.W., Merrill, A.E., Zawack, K., Westphall, M.S.,  
531 Schroeder, F.C., Kimble, J., Coon, J.J., 2015. NeuCode Labeling in Nematodes: Proteomic and  
532 Phosphoproteomic Impact of Ascaroside Treatment in *Caenorhabditis elegans*. *Mol Cell  
533 Proteomics* 14, 2922-2935.  
534

535 Sakai, N., Iwata, R., Yokoi, S., Butcher, R.A., Clardy, J., Tomioka, M., Iino, Y., 2013. A sexually  
536 conditioned switch of chemosensory behavior in *C. elegans*. *PLoS One* 8, e68676.  
537

538 Seidel, S.A., Wienken, C.J., Geissler, S., Jerabek-Willemsen, M., Duhr, S., Reiter, A., Trauner,  
539 D., Braun, D., Baaske, P., 2012. Label-free microscale thermophoresis discriminates sites and  
540 affinity of protein-ligand binding. *Angew Chem Int Ed Engl* 51, 10656-10659.  
541

542 Serrano, R.L., Kuhn, A., Hendricks, A., Helms, J.B., Sinning, I., Groves, M.R., 2004. Structural  
543 analysis of the human Golgi-associated plant pathogenesis related protein GAPR-1 implicates  
544 dimerization as a regulatory mechanism. *J Mol Biol* 339, 173-183.  
545

546 Shang, X., Marchioni, F., Sipes, N., Evelyn, C.R., Jerabek-Willemsen, M., Duhr, S., Seibel, W.,  
547 Wortman, M., Zheng, Y., 2012. Rational design of small molecule inhibitors targeting RhoA  
548 subfamily Rho GTPases. *Chem Biol* 19, 699-710.  
549

550 Shikamoto, Y., Suto, K., Yamazaki, Y., Morita, T., Mizuno, H., 2005. Crystal structure of a CRISP  
551 family Ca<sup>2+</sup> -channel blocker derived from snake venom. *J Mol Biol* 350, 735-743.  
552

553 Srinivasan, J., von Reuss, S.H., Bose, N., Zaslaver, A., Mahanti, P., Ho, M.C., O'Doherty, O.G.,  
554 Edison, A.S., Sternberg, P.W., Schroeder, F.C., 2012. A modular library of small molecule signals  
555 regulates social behaviors in *Caenorhabditis elegans*. *PLoS Biol* 10, e1001237.

556

557 Tarr, G.E., Fairbairn, D., 1973. Conversion of ascaroside esters to free ascarosides in fertilized  
558 eggs of *Ascaris suum* (nematoda). *J Parasitol* 59, 428-433.

559

560 Tarr, G.E., Schnoes, H.K., 1973. Structures of ascaroside aglycones. *Arch Biochem Biophys* 158,  
561 288-296.

562 van Galen, J., Olrichs, N.K., Schouten, A., Serrano, R.L., Nolte-'t Hoen, E.N., Eerland, R.,  
563 Kaloyanova, D., Gros, P., Helms, J.B., 2012. Interaction of GAPR-1 with lipid bilayers is regulated  
564 by alternative homodimerization. *Biochim Biophys Acta* 1818, 2175-2183.

565

566 Van Galen, J., Van Balkom, B.W., Serrano, R.L., Kaloyanova, D., Eerland, R., Stuven, E., Helms,  
567 J.B., 2010. Binding of GAPR-1 to negatively charged phospholipid membranes: unusual binding  
568 characteristics to phosphatidylinositol. *Mol Membr Biol* 27, 81-91.

569

570 Wang, J., Shen, B., Guo, M., Lou, X., Duan, Y., Cheng, X.P., Teng, M., Niu, L., Liu, Q., Huang,  
571 Q., Hao, Q., 2005. Blocking effect and crystal structure of natrin toxin, a cysteine-rich secretory  
572 protein from *Naja atra* venom that targets the BKCa channel. *Biochemistry* 44, 10145-10152.

573

574 Wang, Y.L., Kuo, J.H., Lee, S.C., Liu, J.S., Hsieh, Y.C., Shih, Y.T., Chen, C.J., Chiu, J.J., Wu,  
575 W.G., 2010. Cobra CRISP Functions as an Inflammatory Modulator via a Novel Zn<sup>2+</sup>- and  
576 Heparan Sulfate-dependent Transcriptional Regulation of Endothelial Cell Adhesion Molecules. *J  
577 Biol Chem* 285, 37872-37883.

578

579 Xu, X., Francischetti, I.M., Lai, R., Ribeiro, J.M., Andersen, J.F., 2012. Structure of protein having  
580 inhibitory disintegrin and leukotriene scavenging functions contained in single domain. *J Biol  
581 Chem* 287, 10967-10976.

582

583 Zhan, B., Liu, Y., Badamchian, M., Williamson, A., Feng, J., Loukas, A., Hawdon, J.M., Hotez,  
584 P.J., 2003. Molecular characterisation of the *Ancylostoma*-secreted protein family from the adult  
585 stage of *Ancylostoma caninum*. *Int J Parasitol* 33, 897-907.

586

587 Zillner, K., Jerabek-Willemsen, M., Duhr, S., Braun, D., Langst, G., Baaske, P., 2012. Microscale  
588 thermophoresis as a sensitive method to quantify protein: nucleic acid interactions in solution.  
589 *Methods Mol Biol* 815, 241-252.

590

591

592 **Figure Legends**

593

594 **Figure 1. Targeted ascarosides and their fatty acid side moieties.** The corresponding  
595 ascarosides are ascr#3 (1); oscr#10 (2) and their side chain moieties are 3-5. Compound names are  
596 3 = (R)-8-hydroxynonanoic acid, 4 = (R,E)-8-hydroxynon-2-enoic acid, and 5 = 9-  
597 hydroxynonanoic acid.

598

599 **Figure 2. Synthesis of ascarosides.** The synthetic pathway designed for protected ascarylose 8,  
600 ascr#3 (1), oscr#10 (2) are illustrated.

601

602 **Figure 3. Na-ASP-2 binds both cholesterol and free palmitic acid.** (A) Ligand binding of [<sup>3</sup>H]-  
603 cholesterol to Na-ASP-2. Data represent mean  $\pm$  SD of 3 independent experiments. (B)  
604 Competitive binding of unlabeled cholesterol (50 or 5000 pmol) to Na-ASP-2. Each data point is  
605 the average of duplicate assays and represents the amount of [<sup>3</sup>H]-cholesterol bound relative to a  
606 control containing no unlabeled cholesterol. (C) Ligand binding of [<sup>3</sup>H]-palmitic acid to Na-ASP-  
607 2. (D) Competitive binding of unlabeled palmitic acid (50 or 5000 pmol) to Na-ASP-2. Each data  
608 point is the average of duplicate assays and represents the amount of [<sup>3</sup>H]-palmitic acid bound  
609 relative to a control containing no unlabeled palmitic acid. Data represent mean  $\pm$  SD of 3  
610 independent experiments. Asterisks denote statistical significance relative to the control containing  
611 only the radiolabeled ligand and either purified Na-ASP-2 or Pry1. (\*\*, p < 0.001; \*, p < 0.01).

612

613

614 **Figure 4. Binding of ascarosides to Na-ASP-2 and Pry1.** (A) Free fatty acids and ascarosides  
615 fail to compete with [<sup>3</sup>H]-cholesterol for binding to Na-ASP-2. (B) Free fatty acids and ascarosides

616 compete with [<sup>3</sup>H]-palmitic acid for binding to *Na*-ASP-2. (C) Free fatty acids but not ascarosides  
617 compete [<sup>3</sup>H]-palmitic acid for binding to Pry1. Competitive binding was tested with either 50 or  
618 500 pmol of the unlabeled ligands and 50 pmol of [<sup>3</sup>H]-palmitic acid for binding to 100 pmol  
619 purified *Na*-ASP-2 or Pry1. The ascarosides tested are (1) (ascr#3) and (2) (oscr#10) while the  
620 fatty acids are 3 ((R)-8-hydroxynonanoic acid), 4 ((R,E)-8-hydroxynon-2-enoic acid), and 5 (9-  
621 hydroxynonanoic acid). Data represent mean  $\pm$  SD of 3 independent experiments. Asterisks denote  
622 statistical significance relative to the control containing only the radiolabeled ligand and either  
623 purified *Na*-ASP-2 or Pry1. (\*\*, p < 0.001; \*, p < 0.01). n.s.; not significant.

624

625 **Figure 5. *Na*-ASP-2 selectively binds ascr#3 but not oscr#10.** Binding of ascarosides and their  
626 fatty acid moieties by Pry1 and *Na*-ASP-2 as measured by microscale thermophoresis. (A,  
627 G) Palmitic acid; (B, H) ascr#3; (C, I) oscr#10; (D, J) (R)-8-hydroxynonanoic acid; (E, K) (R,E)-  
628 8-hydroxynon-2-enoic acid; (F, L) 9-hydroxynonanoic acid. Pry1 binds palmitic acid and free  
629 hydroxylated nanonoic acids with similar affinities but binds neither the ascarosides ascr#3 and  
630 oscr#10. *Na*-ASP-2 binds palmitic acid, ascr#3 and free hydroxylated nanonoic acids with similar  
631 affinities but not oscr#10. The Kd values are indicated in each figure with NA (not applicable)  
632 where there is no binding.

633

634 **Figure 6. Comparison of fatty acid binding cavities of *Na*-ASP-2 and Pry1.** (A) Structure based  
635 alignment of *Na*-ASP-2, Pry1 and three *N. brasiliensis* SCP/TAPs proteins (genbank codes  
636 VDL79275.1; VDL83979.1; and VDL79274.1). The sequences are aligned with clustalWOmega  
637 and the secondary structural features are illustrated with the coordinates of HpVAL-4 and Pry1  
638 using ESPript. (Gouet et al., 2003) The alpha helices (alpha 1 and alpha 3) that form the palmitate-

639 binding cavity have similar lengths for *Na*-ASP-2 and the *N. brasiliensis* proteins whereas Pry1 has  
640 shorter helices. The secondary structure elements shown are alpha helices ( $\alpha$ ),  $\beta$ <sub>10</sub>-helices ( $\eta$ ), beta  
641 strands ( $\beta$ ), and beta turns (TT). Identical residues are shown in solid red, and conserved residues  
642 are in red. The locations of the cysteine residues involved in disulfide bonds are numbered in green.  
643 (B) Both of the helices ( $\alpha$ 1 and  $\alpha$  3) forming the palmitic acid binding cavity of Pry1 (cyan) are  
644 shorter than those from *Na*-ASP-2 (gray). Also shown in magenta is the stick structure of palmitate  
645 superposed from the structure of the complex of tablycin-15 with palmitate.

646

Figure 1

bioRxiv preprint doi: <https://doi.org/10.1101/2020.08.07.224964>; this version posted August 7, 2020. The copyright holder for this preprint (which was not certified by peer review) is the author/funder, who has granted bioRxiv a license to display the preprint in perpetuity. It is made available under aCC-BY-NC-ND 4.0 International license.

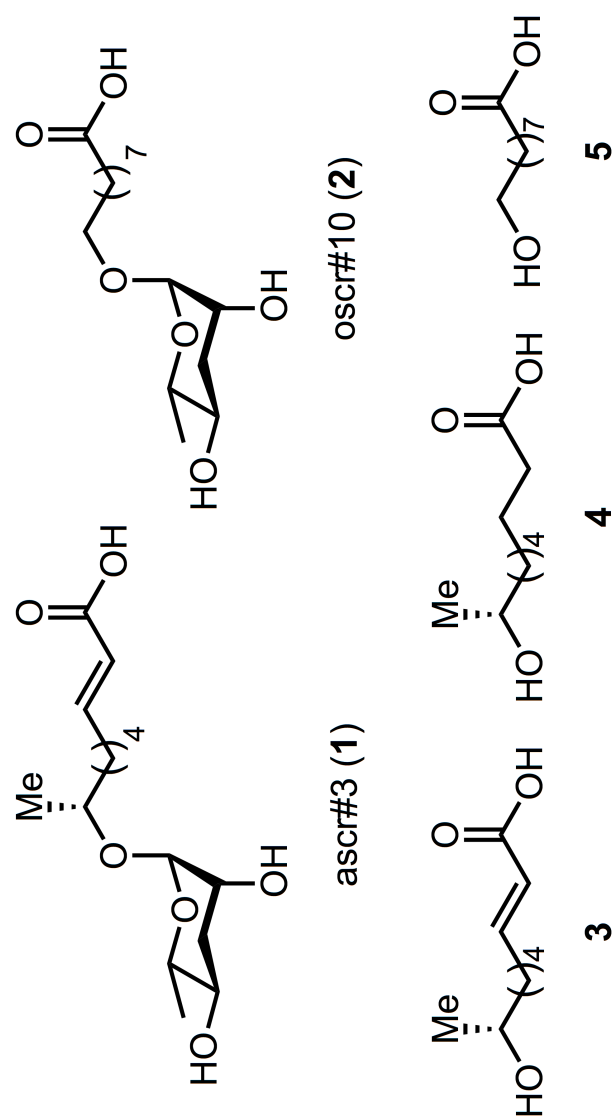
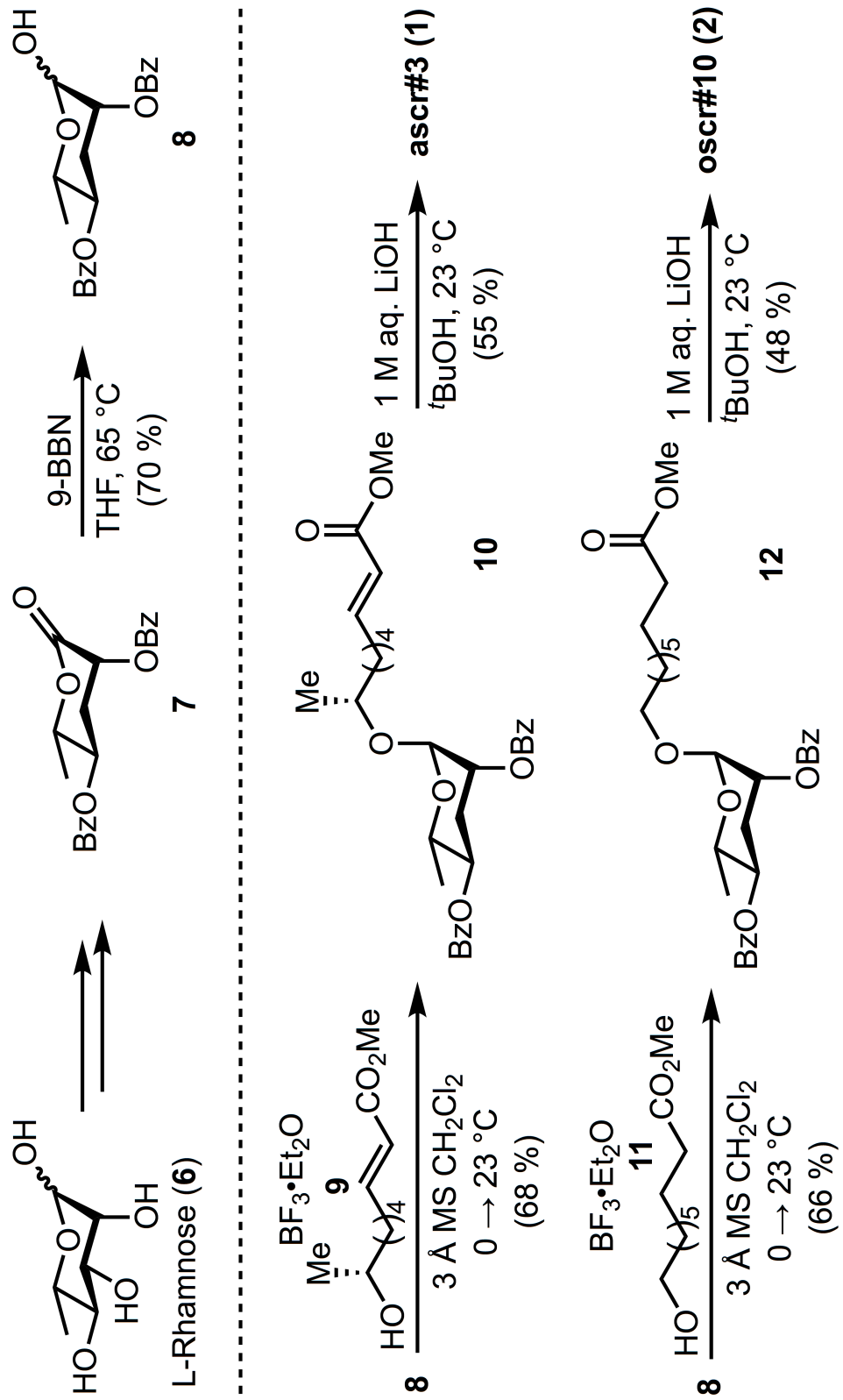


Figure 2

bioRxiv preprint doi: <https://doi.org/10.1101/2020.08.07.224964>; this version posted August 7, 2020. The copyright holder for this preprint (which was not certified by peer review) is the author/funder, who has granted bioRxiv a license to display the preprint in perpetuity. It is made available under aCC-BY-NC-ND 4.0 International license.



bioRxiv preprint doi: <https://doi.org/10.1101/2020.08.07.224964>; this version posted August 7, 2020. The copyright holder for this preprint (which was not certified by peer review) is the author/funder, who has granted bioRxiv a license to display the preprint in perpetuity. It is made available under aCC-BY-NC-ND 4.0 International license.

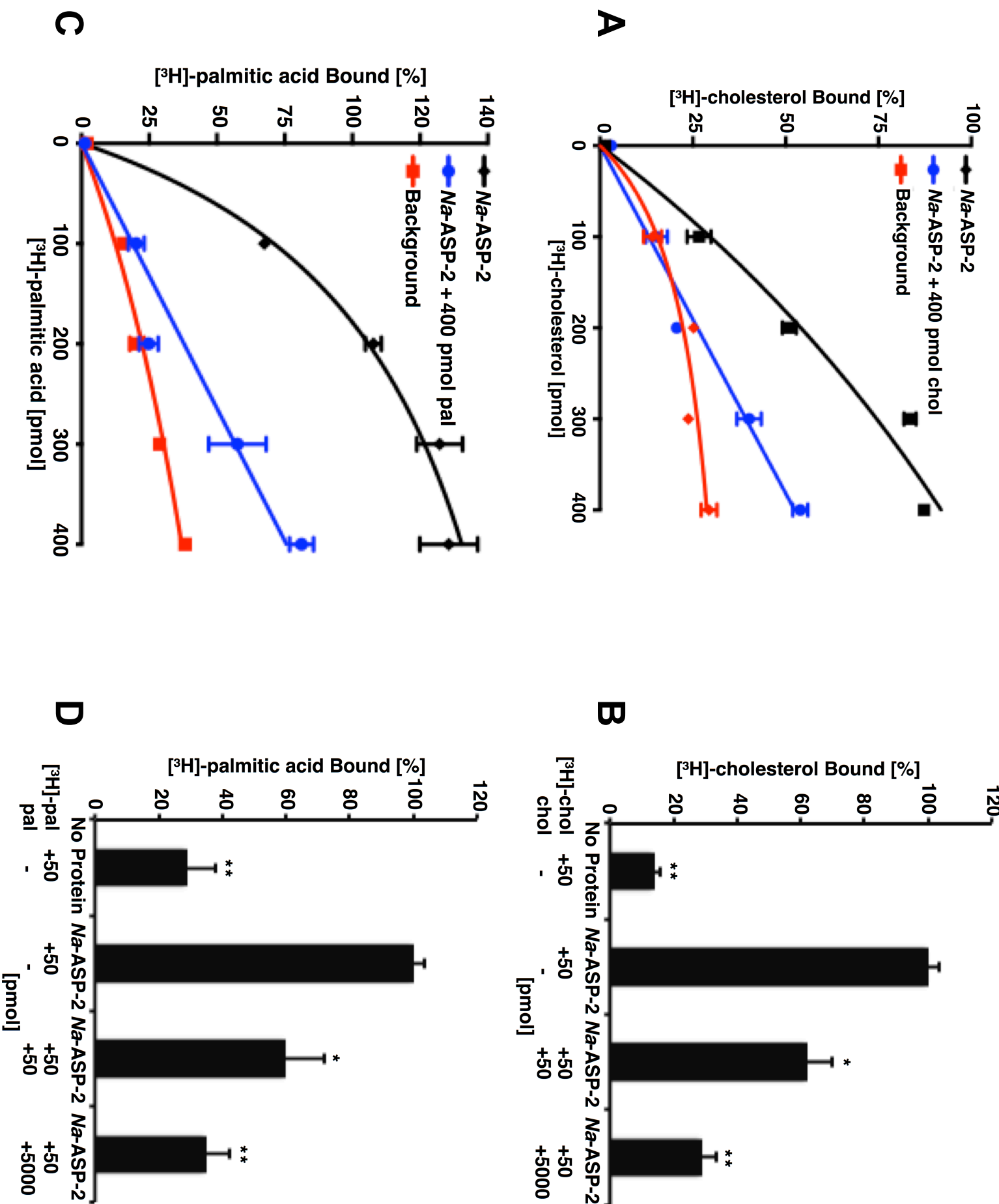
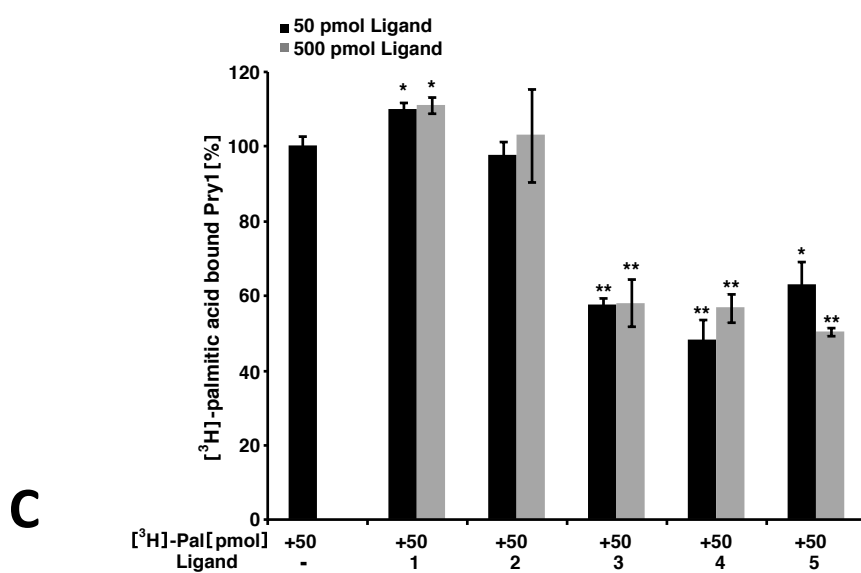
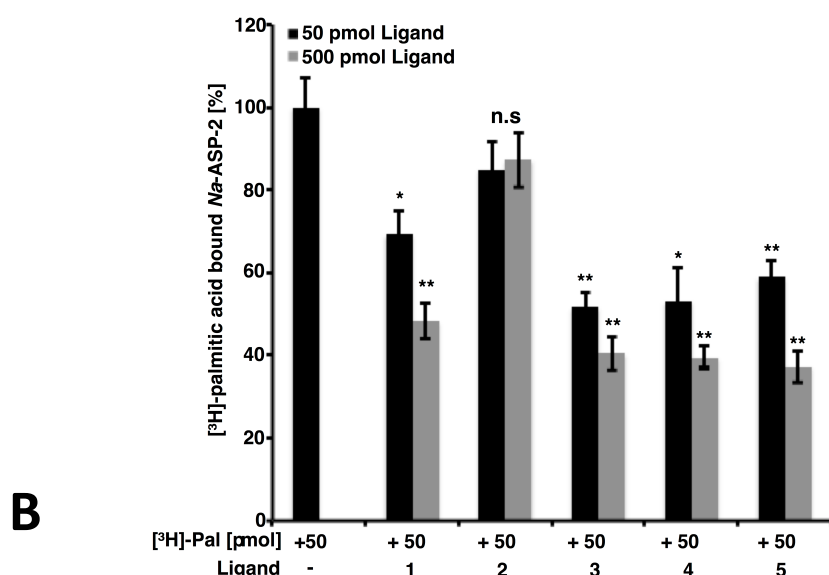
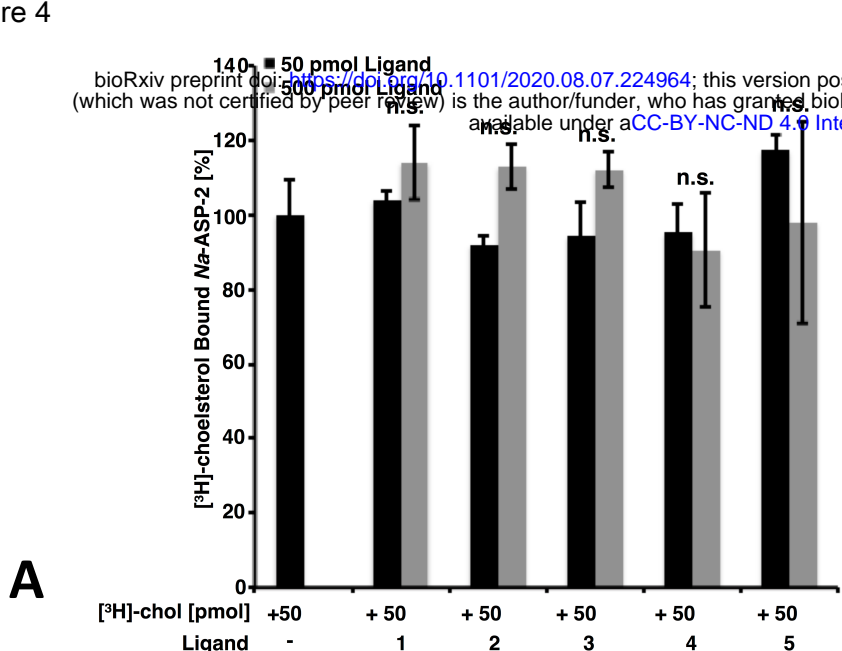


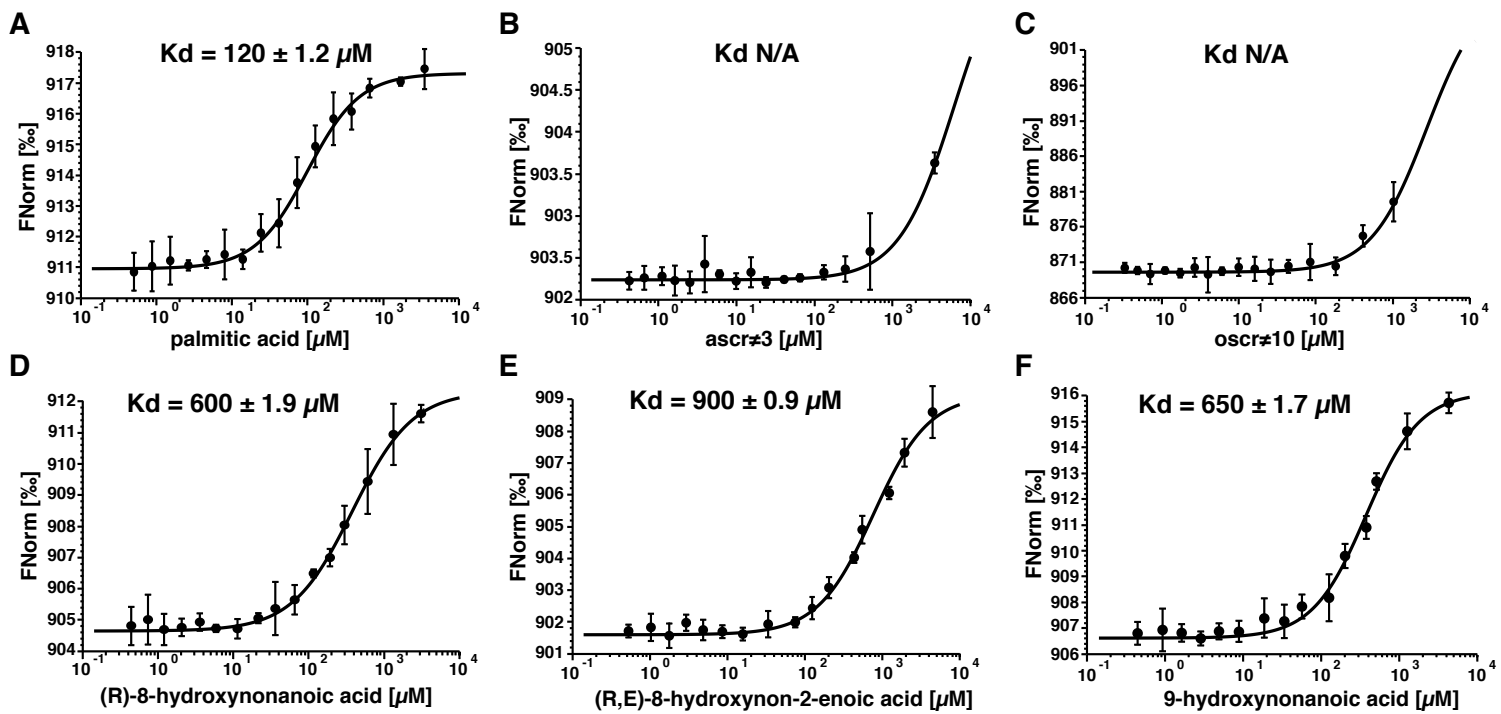
Figure 4

bioRxiv preprint doi: <https://doi.org/10.1101/2020.08.07.224964>; this version posted August 7, 2020. The copyright holder for this preprint (which was not certified by peer review) is the author/funder, who has granted bioRxiv a license to display the preprint in perpetuity. It is made available under aCC-BY-NC-ND 4.0 International license.



bioRxiv preprint doi: <https://doi.org/10.1101/2020.08.07.224964>; this version posted August 7, 2020. The copyright holder for this preprint (which was not certified by peer review) is the author/funder, who has granted bioRxiv a license to display the preprint in perpetuity. It is made available under aCC-BY-NC-ND 4.0 International license.

## Pry1



## Na-ASP-2

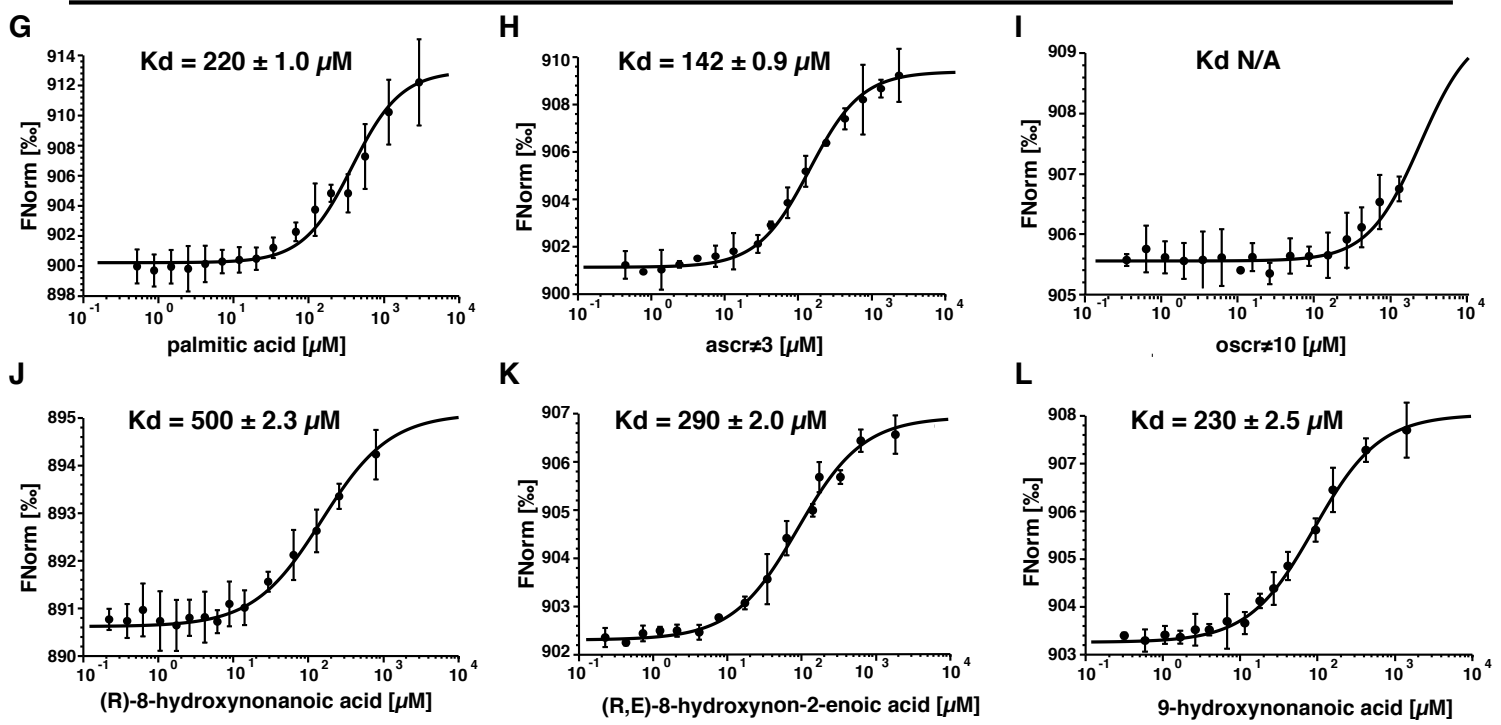


**Figure 5**

bioRxiv preprint doi: <https://doi.org/10.1101/2020.08.07.224964>; this version posted August 7, 2020. The copyright holder for this preprint (which was not certified by peer review) is the author/funder, who has granted bioRxiv a license to display the preprint in perpetuity. It is made available under aCC-BY-NC-ND 4.0 International license.

